PHOSPHORYLATION OF GFAP IS ASSOCIATED WITH INJURY IN THE NEONATAL PIG HYPOXIC-ISCHEMIC BRAIN

Susan M. Sullivan[1], Robert K. P. Sullivan[2], Stephanie M. Miller[1], Zoe Ireland[1], S. Tracey Björkman[1], *David V. Pow[1,3] and *Paul B. Colditz[1]

[1] The University of Queensland, UQ Centre for Clinical Research and Perinatal Research Centre, Herston, Brisbane, QLD, 4029, Australia.

[2] The University of Queensland, Queensland Brain Institute, St Lucia, Brisbane, QLD, 4072, Australia.

[3] School of Medical Sciences and Research Innovations Institute, RMIT, Melbourne, Victoria 3083, Australia.

*Denotes equal contribution from Senior Authors.

Corresponding Author: Susan M. Sullivan. Tel +(617)33466010. Fax +(617)33465594. Email: susan.sullivan@uq.edu.au

Number of Figures: 9

Number of Tables: 4

Abstract

Glial fibrillary acidic protein (GFAP) is an intermediate filament protein expressed in the astrocyte cytoskeleton that plays an important role in the structure and function of the cell. GFAP can be phosphorylated at six serine (Ser) or threonine (Thr) residues but little is known about the role of GFAP phosphorylation in physiological and pathophysiological states. We have generated antibodies against two phosphorylated GFAP (pGFAP) proteins: p8GFAP, where GFAP is phosphorylated at Ser-8 and p13GFAP, where GFAP is phosphorylated at Ser-13. We examined p8GFAP and p13GFAP expression in the control neonatal pig brain and at 24h and 72h after an hypoxic-ischemic (HI) insult. Immunohistochemistry demonstrated pGFAP expression in astrocytes with an atypical cytoskeletal morphology, even in control brains. Semi-quantitative western blotting revealed that p8GFAP expression was significantly increased at 24h post-insult in HI animals with seizures in frontal, parietal, temporal and occipital cortices. At 72h post-insult, p8GFAP and p13GFAP expression were significantly increased in HI animals with seizures in brain regions that are vulnerable to cellular damage (cortex and basal ganglia), but no changes were observed in brain regions that are relatively spared following an HI insult (brain stem and cerebellum). Increased pGFAP expression was associated with poor neurological outcomes such as abnormal encephalography (EEG) and neurobehaviour, and increased histological brain damage. Phosphorylation of GFAP may play an important role in astrocyte remodelling during development and disease and could potentially contribute to the plasticity of the central nervous system.

Introduction

Astrocytes are the key supporting cells in the brain and their function is critical for normal brain activity. Astrocytes provide the link between blood vessels and neurons, and regulate molecules such as neurotransmitters, energy sources, water and ions. Glial fibrillary acidic protein (GFAP) is a type III intermediate filament protein expressed by subsets of grey and white matter astrocytes throughout the central nervous system (CNS) [1]. GFAP knockout mice are more susceptible to brain damage caused by trauma or ischemia than wild-type mice [2-4]. 63% of astrocytes from GFAP knockout mice have altered morphology (short, less branched processes) compared with wild type astrocytes [2]. GFAP is undoubtedly an important protein: 76 GFAP gene mutations have been associated with the rare but fatal neurodegenerative condition Alexander disease [5]. Changes in GFAP mRNA or protein expression have been associated with diseases such as Alzheimer's disease, Creutzfeldt-Jacob disease, Downs Syndrome, stroke, traumatic brain injury, and amyotrophic lateral sclerosis [1,5]. Like other intermediate filament proteins, GFAP plays an important role in determining the shape of the cell and can also influence glutamate homeostasis: Our previous studies have shown that GFAP (via NHERF1 and ezrin) anchors the glutamate transporter GLAST in the plasma membrane, enhancing glutamate transport [6].

GFAP can be phosphorylated at multiple sites, including Thr-7, Ser-8, Ser-13, Ser-17, Ser-34/38 and Ser-389. These six amino acid residues are highly conserved among species, implying the biological importance of GFAP phosphorylation [7]. Enzymes including protein kinase A (PKA), protein kinase C (PKC), calcium/calmodulin dependent protein kinase II (CaMKII), Rho kinase, cleavage furrow (CF) kinase and Cdc2 kinase modulate the phosphorylation of one or more of the GFAP residues [8-12]. Phosphorylation in the N-terminal region (head domain) affects GFAP assembly and in the C-terminal region (tail domain), phosphorylation of Ser-389 affects interactions between GFAP and other intermediate filaments or proteins [10]. Phosphorylation of GFAP causes disassembly of the intermediate filaments and conversely, dephosphorylation (by phosphatase)

restores its ability to polymerize [8]. Various knock-in mice have been created that replace three to five of the six GFAP phosphorylation sites with an alanine residue [7]. When five Ser/Thr residues in the head domain were replaced with alanine residues, there was a significant decrease in GFAP immunoreactivity in most brain regions and the filamentous structures of GFAP were lost in long processes. When Ser-13, Ser-17 and Ser-38 were replaced, there was a slight decrease in GFAP immunoreactivity and labelling was associated with astrocytes with short processes [7]. The integrity of the cytoskeleton is essential for normal astrocyte function, thus GFAP phosphorylation may be an important regulatory mechanism in CNS plasticity during development or in disease conditions.

Hypoxia-ischemia (HI, reduced oxygen availability and/or blood supply) commonly occurs during parturition. HI triggers a cascade of biochemical and molecular events that initially involve decreased energy, glucose and pH, ionic imbalance and glutamate release [13]. After reperfusion, oxygen levels may be restored but the brain remains vulnerable to further injury that can be perpetuated by multiple biological pathways, commonly referred to as secondary energy failure [14]. Neuronal and glial cells die as a result of one or more cell death pathways, for example, excitotoxicity, oxidative stress, cellular oedema and inflammation [15]. This brain damage develops over a period of days to weeks; therefore, a therapeutic window exists for treatment or intervention [16].

In response to CNS insult or injury, astrocytes commonly undergo reactive gliosis, upregulating GFAP and infiltrating areas where neurons are damaged, creating a glial scar [17]. There is increasing evidence that reactive gliosis and glial scar formation are beneficial for the repair of the injured brain [18-20]. The glial scar borders severely damaged tissue, creating a barrier against inflammatory cells and neurotoxic agents and facilitating recovery processes such as blood-brain barrier repair and stabilizing the balance of ions and neurotransmitters in the extracellular space.

Astrocytes play an important role in the ischemic brain [21] but we believe that the gliosis described in rodent studies (for example [22]) occurs at a later time point in the pig HI model. This theory is supported by Martin et al. [23] who demonstrated a significant increase in GFAP immunoreactivity in the HI pig brain at 96h post-insult. Our previous studies have demonstrated that the post-HI brain undergoes significant changes in the expression of various astrocytic and neuronal proteins and the structure of grey and white matter astrocytes [6,24-29]. We have demonstrated pre-gliotic astrocyte changes are evident from 1-8h after an HI insult, prior to histological evidence of neuronal damage [6,29]. At 72h post-insult, overall astrocyte size decreased by 30-40% in grey and white matter and these astrocytic changes were associated with histological brain damage [6,28]. Our results and others confirm the importance of neuron-glia interactions in normal brain function [30].

The post-HI brain is vulnerable to excitotoxicity due to the loss of the glutamate transporters GLAST and GLT-1, which would lead to an accumulation of glutamate in the synapse [24]. High levels of extracellular glutamate and intracellular calcium stimulate phosphorylation of GFAP [31]. Our piglet HI model is ideal for investigating GFAP phosphorylation as some animals develop post-HI seizures, which would further increase levels of glutamate in the extracellular space. In this study, we have investigated whether GFAP phosphorylation is altered after HI insults. We studied the expression of two phosphorylated GFAP (pGFAP) proteins, p8GFAP and p13GFAP, where GFAP is phosphorylated at Ser-8 and Ser-13, respectively. We have used a clinically-relevant animal model: The neonatal pig model of HI produces similar outcomes to human HI infants in terms of the regions of the brain that are damaged (cortex and hippocampus) and the presentation of seizures in some individuals. High levels of extracellular glutamate and intracellular calcium stimulate GFAP phosphorylation, and since both of these occur in the cascade of events after an HI insult, we hypothesised that there would be increased levels of pGFAP in HI brains.

Materials and methods

All studies were approved by the University of Queensland Animal Ethics Committee and experiments were carried out in accordance with NHMRC (Australia) guidelines. Adequate measures were taken to minimise pain or discomfort to animals.

Generation of antibodies

Polyclonal antibodies were generated in New Zealand White rabbits and Sprague Dawley rats against p8GFAP, p13GFAP and the non-phosphorylated form of GFAP, using protocols previously described [32]. Amino acids 3-13 of human GFAP (GenBank #P14136) were selected to create antibodies against, as Ser-8 and Ser-13 are known phosphorylation sites [31]. The unique peptides RRRITpSAARRS for p8GFAP, RRRITSAARRpS for p13GFAP and RRRITSAARRS for the non-phosphorylated form of GFAP were synthesised by GL Biochem (Shanghai, China). As per previously published methods [33,34], dot blots were initially performed to assess the specificity of the antibodies. Further characterisation of the antibodies was performed using western blotting, as detailed below.

Animals

Forty-six newborn Large White pigs were obtained from The University of Queensland Gatton piggery. In the 24h group (N=23), there were seven controls and 16 HI animals, of which seven developed post-HI seizures. In the 72h group (N=23), there were six controls and 17 HI animals, of which eight developed post-HI seizures. To eliminate any confounding effects of anticonvulsant drugs, animals that developed seizures were not treated in this study.

Animal Experiments

Animals were anaesthetised, ventilated and physiological variables monitored as previously described [35,36]. In brief, pigs were rendered hypoxic by decreasing the inspired oxygen (iO_2) to

4% for 30min. Hypotension (ischemia) was induced for the final 10min of the insult by reducing iO_2 until the mean arterial blood pressure (MABP) was <70% of the baseline (~30mm Hg). Littermate controls (N=13) underwent anaesthesia only. Electroencephalography (EEG) was recorded (BRM2; BrainZ Instruments, Auckland, NZ) each day post-insult and neurobehavioural scoring was performed at 8h, 12h, 16h, 24h, 48h and 72h post-insult. Nine behavioural items were assessed as normal (2), moderately abnormal (1), or definitely pathologic (0), with a maximum score of 18 representing normal neurobehaviour.

Animals were euthanased at 24h or 72h post-insult by an overdose of sodium pentobarbital (Lethabarb, 100 mg/kg, I.P.). Brains were removed and 3mm-thick coronal slices prepared. Slices from the right hemisphere were fixed by immersion for 16h in 4% paraformaldehyde in 0.1M phosphate buffer (pH 7.2). Slices from the left hemisphere were further dissected into regions of interest (frontal, parietal, temporal and occipital cortices, basal ganglia, thalamus, hippocampus, brain stem and cerebellum) and frozen in 0.32M sucrose.

Histology

Brain slices were dehydrated, cleared in xylene and embedded in paraffin wax. Tissue sections (4μm) were cut on a rotary microtome and stained with haematoxylin and eosin to assess cellular brain damage. Sections were graded 0-10 based on the highest level of damage observed in a region and the percentage area this lesion occupied (Table 1). Two non-adjacent sections from each region (frontal, parietal, temporal and occipital cortices, basal ganglia, hippocampus, thalamus and cerebellum) were scored by blinded observers (ZI and SS). Sections from the same animal were scored non-sequentially to avoid bias and the average was taken from these scores. The total histology score was represented as a scaled average, with 100 indicating that all regions examined scored the most severe grade of 10.

Western blotting

Protein samples were created by homogenizing the tissue in a 10x volume of ice-cold ddH$_2$O. Samples were spun at 1,400 x *g* at 4°C and the supernatant retained. Protein concentrations were estimated by bicinchoninic acid (BCA) assay (Thermo Fisher Scientific, Scoresby, Australia). Brain homogenates were subjected to 10% SDS-polyacrylamide gel electrophoresis (SDS-PAGE) and then transferred to PVDF membrane. For quantification studies, a protein standard was included on every gel to control for inter-assay variability. The standard was created by pooling 100μL of protein sample made from each brain region from all pigs studied. Membranes were blocked for 1h in 1% skim milk powder in tris-buffered saline-Tween (TBST; 137mM NaCl, 2.7mM KCl, 19mM Tris, 0.1% Tween-20) with agitation and incubated overnight at 4°C with the primary antibody diluted 1:15,000 (p8GFAP and p13GFAP). The membranes were washed in TBST and the anti-rabbit secondary antibody IgG-peroxidase conjugate (Sigma, Castle Hill, Australia) was diluted 1:30,000 in 1% skim milk powder in TBST, added to the membranes and incubated for 1h. The membranes were washed, ECL+ reagent (GE Healthcare, Sydney, Australia) was applied to the membranes and the blots exposed to X-ray film and developed. Membranes were incubated for 1h in stripping buffer (0.2M glycine, 3.47mM SDS, 1% Tween-20, pH 2.2) at 55°C with gentle agitation and then rinsed in TBST, ECL+ applied and re-exposed to film to ensure antibodies were effectively removed. Immunoblotting was performed as above for GFAP using the primary antibody at 1:400,000 (Rabbit anti-GFAP; DakoCytomation, Glostrup, Denmark).

Specificity of the p8GFAP and p13GFAP antibodies was tested using western blotting. In this instance, the primary antibody solution was replaced by a pre-absorbed primary antibody solution. This solution was created using a BSA conjugate supplemented with 0.2M glycine (50μL per 1.1mL of conjugate). 500μL of conjugate was added per 10mL of blocking solution and the primary antibody was diluted at 1:15,000. The pre-absorbed solution was incubated overnight at 4°C with agitation before using on the membrane.

Western blotting and dephosphorylation treatment were used to further examine the specificity of the p8GFAP and p13GFAP antibodies. Protein homogenates were electrophoresed, transferred to PVDF membrane and blocked in 1% skim milk powder in TBST. The membrane to be dephosphorylated was placed in buffer (100mM NaCl, 50mM Tris-HCl, 10mM MgCl2, 1mM dithiothreitol) with 2mL of 5mg/mL alkaline phosphatase (Sigma, Castle Hill, Australia) and incubated for 16h at 37°C with gentle agitation. Western blotting, detection of pGFAP, stripping of membranes and detection of GFAP was performed as above.

Immunohistochemistry

Tissue slices for pGFAP immunohistochemistry were further fixed in 4% paraformaldehyde supplemented with 0.25% glutaraldehyde for 3h. Tissues were embedded in warm 4% agarose and 50μm-thick sections were cut with a vibrating microtome. Sections were incubated in 3% H_2O_2 to in 0.1M sodium phosphate buffer (PBS, pH 7.2) to inhibit endogenous peroxidases and then blocked in 0.5% BSA/0.05% saponin/0.05% sodium azide in PBS for 30min. Immunohistochemistry for pGFAP was performed using the p8GFAP or p13GFAP rat or rabbit polyclonal antibodies diluted at 1:2,500. GFAP immunohistochemistry was performed using a rabbit polyclonal antibody (DakoCytomation, Glostrup, Denmark) at 1:5,000. Biotinylated or Texas Red-conjugated species-specific secondary antibodies were utilized followed by Streptavidin-FITC for fluorescence visualisation or streptavidin-HRP complex (all reagents from GE Healthcare, Australia) for immunoperoxidase visualisation. Immunoperoxidase labelling was revealed using DAB as a chromagen. Sections for immunofluorescence were stained with the fluorescent dye 4,6-diamidinno-2-phenylidole (DAPI; Sigma, Australia) to selectively label the nuclei of the cells.

Amplitude-integrated EEG (aEEG) scoring system

Five distinct background aEEG patterns have been described in neonatal humans and pigs: Continuous normal voltage (CNV), discontinuous normal voltage (DNV), burst suppression (BS), continuous low voltage (CLV) and flat trace (FT) [37,38]. For analysis, the aEEG recordings were reviewed (by SMM) in Analyze version 1.5 software (BrainZ Instruments Ltd, New Zealand) and scored as per Table 2. The scoring system ranges from 0-5.5, with 0 representing normal aEEG and 5.5 being severely abnormal aEEG. Seizures were defined electrographically as repetitive, rhythmic waveforms (duration >10sec) with distinct beginning and end, and clinically as myoclonic jerks, rhythmic pathologic movements (cycling) or tonic postures.

Data collection, analysis and statistics

Imaging was performed using a Zeiss Axio Imager Z1 microscope with a Zeiss AxioCam MRm Rev.3 or AxioCam HRc digital camera. Composite plates of the TIFF images were generated using Adobe Illustrator CS4. Graphs were created in Prism 5.0c for Mac OS X. Data was analysed using IBM SPSS Statistics v19. Shapiro-Wilk test for normality of data was performed. One-way analysis of variance (ANOVA) with Games-Howell post hoc analysis was used to assess differences between the means of more than two groups if data were normally distributed. Sex differences were examined using a Student's t-test. Non-parametric analyses were employed for data that was non-normally distributed (Spearman correlation or Kruskal-Wallis test with Mann-Whitney U post-hoc analysis). Differences were considered significant if the p-value was less than 0.05.

Results

Characterisation of antibodies

Dot blots confirmed that the p8GFAP and p13GFAP antibodies specifically recognised the GFAP peptide when Ser-8 or Ser-13 was phosphorylated but did not cross-react with each other or recognise the same GFAP peptide sequence without phosphorylation (data not shown). Western

blotting was performed with normal and pre-absorbed p8GFAP or p13GFAP primary antibody solutions to confirm that the 50kDa band detected was specific to p8GFAP or p13GFAP. No band was detected if the primary antibody was omitted or the pre-absorbed solutions were used (Fig. 1). Further western blotting experiments were performed to determine that the pGFAP antibodies were indeed detecting a phosphoprotein (Fig. 2). The p8GFAP antibody failed to detect p8GFAP if the membranes were dephosphorylated. Immunoblotting for GFAP revealed that regular GFAP was detected in both the normal membrane and the dephosphorylated membrane (Fig. 2C). The p13GFAP antibody showed a similar result (data not shown).

Group variables

To determine whether animals developed seizures due to having a more severe HI insult, we examined the insult variables across the six groups – controls, HI and HI animals with seizures (here after referred to as HI-seizure animals) at the two time points (Table 3). All HI animals (four groups) received a similar insult, that is, no significant differences were observed between HI and HI-seizure animals for any variables at their respective time points. As expected, at both time points control animals were statistically different ($p<0.01$) to both the HI and HI-seizure animals in terms of the insult variables. Animals at each time point received a similar insult: No significant differences were detected between the 24h and 72h control, HI or HI-seizure animals. There were no significant sex differences observed for any variables (data not shown).

Cellular localisation of pGFAP

Double immunolabelling was performed to confirm that pGFAP was expressed in astrocytes in the control brain (Fig. 3). The p13GFAP antibody detected a protein specifically expressed in astrocytes (Fig. 3A), which co-localised with GFAP detected using a commercial antibody (Fig. 3B-C). GFAP and pGFAP were differentially expressed in the astrocyte. Expression of pGFAP was concentrated in processes near the cell body, but also expressed in unusual terminal dilations of the

astrocyte processes (arrowhead, Fig. 3D) and parts of the astrocyte process in between (double arrowhead, Fig. 3D). pGFAP expression was also observed in end-feet of astrocytes contacting blood vessels (Fig. 3E). Similar results were observed using the p8GFAP antibody (data not shown).

Expression of pGFAP in control and HI brains with mild or no cellular damage was similar (Fig. 4A-B). Astrocytes expressing pGFAP had abnormal cytoskeletal morphology (Fig. 4). The majority of labeled astrocytes had very short processes. The few astrocytes that expressed pGFAP in long processes had atypical features such as thickened, varicose processes (Fig. 4D) and did not exhibit the fine, bushy processes of a normal control astrocyte (see images contained within [6,39]). Immunolabelling for pGFAP in HI brains with moderate to severe cellular damage (72h post-insult) revealed that pGFAP expression was upregulated (Fig. 4C). In these animals, astrocytes had abnormal cytoskeletal morphology with shortened cell processes (Fig. 4E).

pGFAP in brain homogenates

Semi-quantitative western blotting was performed to examine p8GFAP and p13GFAP expression in nine brain regions from control, HI and HI-seizure animals at 24h and 72h post-insult. Figure 5 shows an example western blot result from three representative animals at 72h post-insult. Expression of p8GFAP was upregulated in HI-seizure animals as shown by the darker, more intense band on the film (Fig. 5).

Figure 6 shows p8GFAP expression at 24h and 72h post-insult in control, HI and HI-seizure animals in nine brain regions: frontal, parietal, temporal and occipital cortices, basal ganglia, thalamus, hippocampus, brain stem and cerebellum. At 24h post-insult, expression of p8GFAP was significantly upregulated in the four cortices in HI-seizure animals compared with controls. HI-seizure animals had significantly increased p8GFAP expression in parietal, temporal and occipital

cortices compared to HI animals. At 72h post-insult, p8GFAP expression was significantly upregulated in the four cortices, basal ganglia and thalamus, when compared with controls. HI-seizure animals had significantly increased p8GFAP expression in frontal, temporal and occipital cortices and thalamus compared with HI animals.

Expression of p13GFAP was not significantly different in any brain region studied at 24h post-insult (Fig. 7). At 72h post-insult, p13GFAP expression was significantly upregulated in the four cortices and basal ganglia, when compared with controls. HI-seizure animals had significantly increased p13GFAP expression in the four cortices compared with HI animals. HI animals had significantly higher p13GFAP expression compared with controls in basal ganglia only (indicated by § in Fig. 7E). In the thalamus, there was a trend towards increased p13GFAP expression in HI-seizure animals at 72h post-insult, but this was not significant across the three groups ($p=0.058$). Western blots for p8GFAP and p13GFAP were routinely stripped and re-probed with anti-GFAP antibody. GFAP expression was not significantly different across groups for any brain region at the time points examined (data not shown).

pGFAP expression and brain injury

HI triggers a cascade of events that ultimately result in brain damage. We examined which physiological variables had the greatest influence on pGFAP expression. Table 4 lists the Spearman correlation coefficients (r_s) for the significant relationships identified. Animals that had increased pGFAP expression consistently had poor neurobehaviour and aEEG scores post-insult. At 72h post-insult a strong association was identified between p13GFAP expression and aEEG score on day 1 (Fig. 8A). Increased p13GFAP expression was also strongly associated with neurobehaviour score at 48hr (Fig. 8B). Similar relationships were found for p8GFAP. Animals with higher histological injury tended to have higher levels of pGFAP expression. A strong association was identified between cortical p13GFAP expression and the average cortical histology score (Fig. 8C). A similar

relationship existed between the cortical p8GFAP expression and the average cortical histology score at 72h post-insult (r_s=0.600, p=0.002). The relationship between average cortical p8GFAP or p13GFAP expression and histology score (including non-cortical brain regions) was also significant (r_s=0.491, p=0.017 for p8GFAP and r_s=0.655, p=0.001 for p13GFAP).

Discussion

GFAP is a key cytoskeletal protein but little is known about its specific functions. Previous studies have created pGFAP antibodies, some of which are commercially available [40,41]. In this study, we generated and characterised our polyclonal antibodies against p8GFAP and p13GFAP to ensure that they detected only the phosphorylated form of GFAP, and that this phosphoprotein was detectable in astrocytes in the pig brain. Our results demonstrated that pGFAP expression was increased in brain regions that were vulnerable to HI brain damage and that increased pGFAP expression was associated with poor neurological outcomes and histological brain damage.

GFAP can be phosphorylated at multiple sites and this influences the stability of the glial cytoskeleton, however there are very few studies examining the expression of pGFAP in the intact CNS. *In vitro* autoradiography studies have shown increased phosphorylation of GFAP in rat hippocampal slices following HI [42]. Two-dimensional immunoblotting identified an increase in pGFAP isoforms in brains from Alzheimer's disease patients [43]. There is only one other study that has used a phospho-specific GFAP antibody to examine the expression of pGFAP in relation to a CNS disease, and those results support our observations. Using quantitative western blotting, Herskowitz et al. [44] detected an eight-fold increase in p13GFAP in post-mortem brains from individuals with frontotemporal lobe degeneration.

Anatomy of cells expressing pGFAP

There are limited high magnification images detailing the anatomy of pGFAP-expressing astrocytes. We demonstrate that astrocytes expressing pGFAP have atypical cytoskeletal morphology, even in control brains. Our observations of pGFAP-expressing astrocytes with short processes are supported by previous literature [7]. It is likely that remodelling or 'pruning' is occurring our neonatal brains. In both human and rodents, GFAP expression increases with age [45]. Expression of pGFAP has been demonstrated in the adult human brain [44] but further study is required to determine whether GFAP phosphorylation changes with age.

pGFAP expression in the HI brain

We explored the relationships between antemortem variables, histological injury and expression of pGFAP. Although we could not identify a consistent physiological variable that drove phosphorylation of GFAP we consistently observed in that animals with increased p8GFAP in a particular region also had increased p13GFAP (72hr post-insult only). This increased pGFAP expression was associated with poor neurological outcome (aEEG or neurobehaviour score). The association between increased pGFAP expression and histological injury further confirms this relationship. Western blotting showed that increased phosphorylation of GFAP was restricted to regions of the brain that are damaged by an HI insult and pGFAP was not increased in areas that are relatively spared after HI. Our immunohistochemical images support this: In animals with mild or no histological damage (Fig. 4B), the expression of pGFAP was similar to control brains.

Figure 9 indicates where phosphorylation of GFAP might play a role in the events following an HI insult. HI causes a series of initial events (grey boxes) such as decreased pH, ATP and glucose that ultimately result in cell death. Loss of glutamate transporters and seizures exacerbate extracellular accumulation of glutamate, which would contribute to increased cell death via excitotoxicity. This same rise in extracellular glutamate would also stimulate phosphorylation of GFAP, but it is unclear

whether this contributes to increased cell death or is potentially part of a long-term repair/plasticity process.

Since there were no differences observed in the HI and HI-seizure animals in terms of the HI insult variables, it is likely that the development of seizures and increased pGFAP in some HI animals is due to other intrinsic or inter-individual factors. We hypothesized that pGFAP would be increased in HI animals due to the involvement of glutamate in the pathogenesis of HI brain injury. There were trends toward increased pGFAP expression in some brain regions of HI animals but this only reached significance for p13GFAP in basal ganglia at 72h post-insult (a three-fold increase compared with controls). However, when there is additional injury burden and potentially more glutamate release by post-HI seizures, there were large differences between control and HI-seizure animals. We observed a significant two- to three-fold increase in p8GFAP in the cortex at 24h post-insult and a three- to seven-fold increase in p8GFAP and p13GFAP in various brain regions at 72h post-insult compared to controls. To further elucidate the role of seizures in GFAP phosphorylation, pGFAP expression could be examined without HI insult by using a standard kindling model or a status epilepticus model where spontaneous seizures are induced in rodents by electrical stimulation or chemical agents such as kainate or pilocarpine (for review, see [46]).

Timing of increase in pGFAP

GFAP protein expression as detected by western blot was not significantly different across groups for any brain region. Thus the observation of increased pGFAP was independent to the expression of regular GFAP. We have previously observed using immunohistochemistry that GFAP immunoreactivity is decreased in white matter and upregulated in grey matter after HI insults (see [28] Fig. 3A versus 3B). The increased grey matter and decreased white matter GFAP expression may effectively 'cancel' each other out in a cortical protein homogenate sample.

Phosphorylation of GFAP at Ser-8 but not Ser-13 was increased at 24h post-insult. At 72h post-insult, the expression of p8GFAP and p13GFAP was similar, with areas such as cortex and basal ganglia showing increased pGFAP expression. This supports the concept of differential regulation of phosphorylation sites of GFAP. Studies have shown that Ser-8 phosphorylation is regulated by PKA, PKC and cdc2 kinase, while Ser-13 phosphorylation is regulated by PKA, PKC, CaMKII, Rho kinase and CF kinase [47]. Increased phosphorylation at both Ser-8 and Ser-13 could be efficiently caused by increased activity of PKA or PKC but only an increase in cdc2 kinase activity would cause increased GFAP phosphorylation at Ser-8 independent of Ser-13. Alternatively, phosphorylation of GFAP at Ser-8 creates a conformational change that allows subsequent phosphorylation of Ser-13. As phosphorylation is a reversible process, we propose that modulation of kinase activity might represent an interesting therapeutic strategy for future research.

Reactive gliosis and interactions with other proteins

The increase in pGFAP expression could contribute to reactive gliosis by conferring plasticity to the astrocyte cytoskeleton. Geiger et al [48] have described two phases of glial activation in cerebral HIV infection but only increased immunoreactivity of GFAP and ezrin was associated with neuronal damage. Phosphorylation of GFAP may alter the interaction with ezrin and affect glial activation and/or neuronal cell damage. Studies have shown that Ser-8 phosphorylation of GFAP by PKC or cdc2 kinase enhances the interaction between GFAP and 14-3-3γ [49]. The converse is also plausible, that phosphorylation of GFAP disrupts its interactions with other proteins. Our previous studies in the rat and pig brain have shown the link between GFAP and GLAST (via NHERF1, ezrin and potentially other proteins) is important in HI brain injury: Regions of the brain exhibiting this co-association also showed no signs of cellular damage [25]. Future experiments could use immunoprecipitation to determine if phosphorylation of GFAP disrupts these protein interactions, thereby decreasing GLAST-mediated glutamate uptake and enhancing excitotoxic cell death.

Concluding remarks

The role of GFAP phosphorylation in disease is relatively unexplored. We examined the phosphorylation of GFAP at Ser-8 and Ser-13 in control and HI neonatal pig brains. Previous literature [42-44] supports our finding of increased phosphorylation of GFAP, but further research is required to determine whether this is a beneficial or harmful change for the HI brain. Phosphorylation is an energy-dependent process, requiring adenosine triphosphate (ATP) conversion to adenosine diphosphate (ADP) by kinases to phosphorylate the serine or threonine residue. It seems counterproductive to utilise energy to phosphorylate a cytoskeletal protein in an energy-depleted physiological condition such as following HI. The alternative view is that phosphorylation of GFAP may be an essential part of a repair continuum: The astrocyte cytoskeleton is phosphorylated to depolymerise the cytoskeleton so that the astrocyte has increased plasticity and motility to promote survival of astrocytes (and the neurons they support) during the secondary energy failure phase of the disease. Given the vital role of astrocytes in the CNS, further studies of GFAP phosphorylation are required to understand its influence on the glial cytoskeleton in normal development and in diseases that affect the CNS.

The authors declare that they have no conflict of interest.

References

1. Eng LF, Ghirnikar RS, Lee YL (2000) Glial fibrillary acidic protein: GFAP-thirty-one years (1969-2000). Neurochemical Research 25 (9-10):1439-1451. doi:10.1023/a:1007677003387

2. Anderova M, Kubinova S, Mazel T, Chvatal A, Eliasson C, Pekny M, Sykova E (2001) Effect of elevated K(+), hypotonic stress, and cortical spreading depression on astrocyte swelling in GFAP-deficient mice. Glia 35 (3):189-203. doi:10.1002/glia.1084

3. Tanaka H, Katoh A, Oguro K, Shimazaki K, Gomi H, Itohara S, Masuzawa T, Kawai N (2002) Disturbance of hippocampal long-term potentiation after transient ischemia in GFAP deficient mice. Journal of Neuroscience Research 67 (1):11-20. doi:10.1002/jnr.10004

4. Hughes EG, Maguire JL, McMinn MT, Scholz RE, Sutherland ML (2004) Loss of glial fibrillary acidic protein results in decreased glutamate transport and inhibition of PKA-induced EAAT2 cell surface trafficking. Brain Research Molecular Brain Research 124 (2):114-123

5. Middeldorp J, Hol EM (2011) GFAP in health and disease. Progress in Neurobiology 93 (3):421-443. doi:10.1016/j.pneurobio.2011.01.005

6. Sullivan SM, Bjorkman ST, Miller SM, Colditz PB, Pow DV (2010) Structural Remodeling of Gray Matter Astrocytes in the Neonatal Pig Brain After Hypoxia/Ischemia. Glia 58 (2):181-194. doi:10.1002/glia.20911

7. Takemura M, Gomi H, Colucci-Guyon E, Itohara S (2002) Protective role of phosphorylation in turnover of glial fibrillary acidic protein in mice. J Neurosci 22 (16):6972-6979

8. Inagaki M, Gonda Y, Nishizawa K, Kitamura S, Sato C, Ando S, Tanabe K, Kikuchi K, Tsuiki S, Nishi Y (1990) Phosphorylation sites linked to glial filament disassembly in vitro locate in a non-alpha-helical head domain. Journal of Biological Chemistry 265 (8):4722-4729

9. Tsujimura K, Tanaka J, Ando S, Matsuoka Y, Kusubata M, Sugiura H, Yamauchi T, Inagaki M (1994) Identification of phosphorylation sites on glial fibrillary acidic protein for cdc2 kinase and Ca2+-calmodulin-dependent protein-kinase-II. Journal of Biochemistry 116 (2):426-434

10. Inagaki M, Nakamura Y, Takeda M, Nishimura T, Inagaki N (1994) Glial fibrillary acidic protein - Dynamic property and regulation by phosphorylation. Brain Pathology 4 (3):239-243. doi:10.1111/j.1750-3639.1994.tb00839.x

11. Sekimata M, Tsujimura K, Tanaka J, Takeuchi Y, Inagaki N, Inagaki M (1996) Detection of protein kinase activity specifically activated at metaphase anaphase transition. Journal of Cell Biology 132 (4):635-641. doi:10.1083/jcb.132.4.635

12. Kosako H, Goto H, Yanagida M, Matsuzawa K, Fujita M, Tomono Y, Okigaki T, Odai H, Kaibuchi K, Inagaki M (1999) Specific accumulation of Rho-associated kinase at the cleavage furrow during cytokinesis: cleavage furrow-specific phosphorylation of intermediate filaments. Oncogene 18 (17):2783-2788. doi:10.1038/sj.onc.1202633

13. Lipton P (1999) Ischemic cell death in brain neurons. Physiological Reviews 79 (4):1431-1568

14. Ferriero DM (2004) Medical progress - Neonatal brain injury. New England Journal of Medicine 351 (19):1985-1995. doi:10.1056/NEJMra041996

15. Hertz L (2008) Bioenergetics of cerebral ischemia: A cellular perspective. Neuropharmacology 55 (3):289-309. doi:10.1016/j.neuropharm.2008.05.023

16. Cilio MR, Ferriero DM (2010) Synergistic neuroprotective therapies with hypothermia. Seminars in Fetal & Neonatal Medicine 15 (5):293-298. doi:10.1016/j.siny.2010.02.002

17. Pekny M, Wilhelmsson U, Bogestal YR, Pekna M (2007) The role of astrocytes and complement system in neural plasticity. In: Bagetta GCMTLSA (ed) Neuroinflammation in Neuronal Death and Repair, vol 82. International Review of Neurobiology. pp 95-111. doi:10.1016/s0074-7742(07)82005-8

18. Li L, Lundkvist A, Andersson D, Wilhelmsson U, Nagai N, Pardo AC, Nodin C, Stahlberg A, Aprico K, Larsson K, Yabe T, Moons L, Fotheringham A, Davies I, Carmeliet P, Schwartz JP, Pekna M, Kubista M, Blomstrand F, Maragakis N, Nilsson M, Pekny M (2008) Protective role of reactive astrocytes in brain ischemia. Journal of Cerebral Blood Flow and Metabolism 28 (3):468-481. doi:10.1038/sj.jcbfm.9600546

19. Jarlestedt K, Rousset CI, Faiz M, Wilhelmsson U, Stahlberg A, Sourkova H, Pekna M, Mallard C, Hagberg H, Pekny M (2010) Attenuation of Reactive Gliosis Does Not Affect Infarct Volume in Neonatal Hypoxic-Ischemic Brain Injury in Mice. Plos One 5 (4). doi:10.1371/journal.pone.0010397

20. Sofroniew MV, Vinters HV (2010) Astrocytes: biology and pathology. Acta Neuropathologica 119 (1):7-35. doi:10.1007/s00401-009-0619-8

21. Dienel GA, Hertz L (2005) Astrocytic contributions to bioenergeties of cerebral ischemia. Glia 50 (4):362-388. doi:10.1002/glia.20157

22. Sizonenko SV, Camm EJ, Dayer A, Kiss JZ (2008) Glial responses to neonatal hypoxic-ischemic injury in the rat cerebral cortex. International Journal of Developmental Neuroscience 26 (1):37-45. doi:10.1016/j.ijdevneu.2007.08.014

23. Martin LJ, Brambrink AM, Lehmann C, PorteraCailliau C, Koehler R, Rothstein J, Traystman RJ (1997) Hypoxia-ischemia causes abnormalities in glutamate transporters and death of astroglia and neurons in newborn striatum. Annals of Neurology 42 (3):335-348. doi:10.1002/ana.410420310

24. Pow DV, Naidoo T, Lingwood BE, Healy GN, Williams SM, Sullivan RKP, O'Driscoll S, Colditz PB (2004) Loss of glial glutamate transporters and induction of neuronal expression of GLT-1B in the hypoxic neonatal pig brain. Developmental Brain Research 153 (1):1-11. doi:10.1016/j.devbrainres.2004.06.019

25. Sullivan SM, Lee A, Bjorkman ST, Miller SM, Sullivan RKP, Poronnik P, Colditz PB, Pow DV (2007) Cytoskeletal anchoring of GLAST determines susceptibility to brain damage - An identified role for GFAP. Journal of Biological Chemistry 282 (40):29414-29423. doi:10.1074/jbc.M704152200

26. Sullivan SM, Macnab LT, Bjorkman ST, Colditz PB, Pow DV (2007) GLAST1b, the EXON-9 skipping form of the glutamate-aspartate transporter EAAT1 is a sensitive marker of neuronal

dysfunction in the hypoxic brain. Neuroscience 149 (2):434-445. doi:10.1016/j.neuroscience.2007.08.011

27. Lingwood BE, Healy GN, Sullivan SM, Pow DV, Colditz PB (2008) MAP2 provides reliable early assessment of neural injury in the newborn piglet model of birth asphyxia. Journal of Neuroscience Methods 171 (1):140-146. doi:10.1016/j.jneumeth.2008.02.011

28. Sullivan SM, Bjorkman ST, Miller SM, Colditz PB, Pow DV (2010) Morphological changes in white matter astrocytes in response to hypoxia/ischemia in the neonatal pig. Brain Research 1319:164-174. doi:10.1016/j.brainres.2010.01.010

29. Lee A, Lingwood BE, Bjorkman ST, Miller SM, Poronnik P, Barnett NL, Colditz P, Pow DV (2010) Rapid loss of glutamine synthetase from astrocytes in response to hypoxia: Implications for excitotoxicity. Journal of Chemical Neuroanatomy 39 (3):211-220. doi:10.1016/j.jchemneu.2009.12.002

30. Hertz L, Zielke HR (2004) Astrocytic control of glutamatergic activity: astrocytes as stars of the show. Trends in Neurosciences 27 (12):735-743. doi:10.1016/j.tins.2004.10.008

31. Rodnight R, Goncalves CA, Wofchuk ST, Leal R (1997) Control of the phosphorylation of the astrocyte marker glial fibrillary acidic protein (GFAP) in the immature rat hippocampus by glutamate and calcium ions: Possible key factor in astrocytic plasticity. Brazilian Journal of Medical and Biological Research 30 (3):325-338

32. Pow DV, Sullivan RKP, H S (2003) Antibody production and immunocytochemical localization of amino acid transporters. Methods Mol Biol 227:213-244.

33. Macnab LT, Williams SM, Pow DV (2006) Expression of the exon 3 skipping form of GLAST, GLASTIa, in brain and retina. Neuroreport 17 (18):1867-1870. doi:10.1097/WNR.0b013e328010b898

34. Williams SM, Diaz CM, Macnab LT, Sullivan RKP, Pow DV (2006) Immunocytochemical analysis of D-serine distribution in the mammalian brain reveals novel anatomical compartmentalizations in glia and neurons. Glia 53 (4):401-411. doi:10.1002/glia.20300

35. Bjorkman ST, Foster KA, O'Driscoll SM, Healy GN, Lingwood BE, Burke C, Colditz PB (2006) Hypoxic/ischemic models in newborn piglet: Comparison of constant FiO(2) versus variable FiO(2) delivery. Brain Research 1100:110-117. doi:10.1016/j.brainres.2006.04.119

36. Bjorkman ST, Miller SM, Rose SE, Burke C, Colditz PB (2010) Seizures are associated with brain injury severity in a neonatal model of hypoxia-ischemia. Neuroscience 166 (1):157-167. doi:10.1016/j.neuroscience.2009.11.067

37. Toet MC, van Rooij LGM, deVries LS (2008) The Use of Amplitude Integrated Electroencephalography for Assessing Neonatal Neurologic Injury. Clinics in Perinatology 35 (4):665-678. doi:10.1016/j.clp.2008.07.017

38. Peeters-Scholte C, van den Tweel E, Ioroj T, Post I, Braun K, Veldhuis W, Nicolay K, Groenendaal F, van Bel F (2002) Pharmacological interventions in the newborn piglet in the first 24 h after hypoxia-ischemia - A hemodynamic and electrophysiological perspective. Experimental Brain Research 147 (2):200-208. doi:10.1007/s00221-002-1182-x

39. Wilhelmsson U, Bushongt EA, Price DL, Smarr BL, Phung V, Terada M, Ellisman MH, Pekny M (2006) Redefining the concept of reactive astrocytes as cells that remain within their unique domains upon reaction to injury. Proceedings of the National Academy of Sciences of the United States of America 103 (46):17513-17518. doi:10.1073/pnas.0602841103

40. Yano T, Taura C, Shibata M, Hirono Y, Ando S, Kusubata M, Takahashi T, Inagaki M (1991) A monoclonal-antibody to the phosphorylated form of glial fibrillary acidic protein - application to a nonradioactive method for measuring protein-kinase activities. Biochemical and Biophysical Research Communications 175 (3):1144-1151. doi:10.1016/0006-291x(91)91685-6

41. Matsuoka Y, Nishizawa K, Yano T, Shibata M, Ando S, Takahashi T, Inagaki M (1992) Two different protein-kinases act on a different time schedule as glial filament kinases during mitosis. Embo Journal 11 (8):2895-2902

42. Valentim LM, Michalowski CB, Gottardo SP, Pedroso L, Gestrich LG, Netto CA, Salbego CG, Rodnight R (1999) Effects of transient cerebral ischemia on glial fibrillary acidic protein phosphorylation and immunocontent in rat hippocampus. Neuroscience 91 (4):1291-1297. doi:10.1016/s0306-4522(98)00707-6

43. Korolainen MA, Auriola S, Nyman TA, Alafuzoff I, Pirttila T (2005) Proteomic analysis of glial fibrillary acidic protein in Alzheimer's disease and aging brain. Neurobiology of Disease 20 (3):858-870. doi:10.1016/j.nbd.2005.05.021

44. Herskowitz JH, Seyfried NT, Duong DM, Xia Q, Rees HD, Gearing M, Peng J, Lah JJ, Levey AI (2010) Phosphoproteomic Analysis Reveals Site-Specific Changes in GFAP and NDRG2 Phosphorylation in Frontotemporal Lobar Degeneration. Journal of Proteome Research 9 (12):6368-6379. doi:10.1021/pr100666c

45. Finch CE (2003) Neurons, glia, and plasticity in normal brain aging. Neurobiology of Aging 24:S123-S127. doi:10.1016/s0197-4580(03)00051-4

46. Morimoto K, Fahnestock M, Racine RJ (2004) Kindling and status epilepticus models of epilepsy: rewiring the brain. Progress in Neurobiology 73 (1):1-60. doi:10.1016/j.pneurobio.2004.03.009

47. Inagaki M, Matsuoka Y, Tsujimura K, Ando S, Tokui T, Takahashi T, Inagaki N (1996) Dynamic property of intermediate filaments: Regulation by phosphorylation. Bioessays 18 (6):481-487. doi:10.1002/bies.950180610

48. Geiger KD, Stoldt P, Schlote W, Derouiche A (2006) Ezrin immunoreactivity reveals specific astrocyte activation in cerebral HIV. Journal of Neuropathology and Experimental Neurology 65 (1):87-96. doi:10.1097/01.jnen.0000195943.32786.39

49. Li H, Guo Y, Teng J, Ding M, Yu ACH, Chen J (2006) 14-3-3 gamma affects dynamics and integrity of glial filaments by binding to phosphorylated GFAP. Journal of Cell Science 119 (21):4452-4461. doi:10.1242/jcs.03219

Table 1: Histology scoring system

Histological changes	Grey Matter	White Matter	Area affected	Grade
None	No abnormal features		0	0
Mild: Damage to individual cells	Abnormal cell morphology, cell lysis, cell shrinkage, chromatin condensation	Cell lysis, cell shrinkage	<10%	1
			10-25%	2
			25-50%	3
			>50%	4
Moderate: Damage in a layer or group of cells	Vacuolation, chromatin condensation, cell lysis, cell death	Vacuolation, poor myelination	<25%	5
			25-50%	6
			>50%	7
Severe: Damage to all cells within a certain area	Features as per moderate damage but <u>no</u> evidence of any healthy cells	Damage to myelinated tracts	<25%	8
			25-50%	9
			>50%	10

Table 2: aEEG scoring system

Background EEG pattern	Seizure activity				
	No Seizures	Epileptiform Activity	Single Seizure	Repetitive Seizures	Status Epilepticus
Continuous normal voltage (CNV)	0	0.5	1	1.5	N/A
Discontinuous normal voltage (DNV)	1	1.5	2	2.5	3
Burst suppression (BS)	2	2.5	3	3.5	4
Continuous low voltage (CLV)	3	3.5	4	4.5	5
Flat trace (FT)	4	4.5	5	5.5	N/A

N/A: Not applicable as these physiological scenarios are unlikely to occur.

Table 3: Insult variables for the six groups in this study

Parameter	24h post-insult			72h post-insult		
	Control	**HI**	**HI Sz**	**Control**	**HI**	**HI Sz**
Body weight (kg)	1.52±0.07	1.61±0.05	1.64±0.13	1.85±0.15	1.6±0.08	1.52±0.07
Insult length (min)	0±0**	32.35±1.69	30.26±1.06	0±0^^	29.41±0.88	31.43±1.70
Time LaEEG (min)	0±0**	24.66±2.70	22.18±2.02	0±0^^	23.25±1.18	25.75±2.22
Time (min) MABP<70%	0±0**	10.65±2.11	11.58±2.51	0±0^^	14.06±2.38	14.2±3.22
Time (min) HR<140bpm	0±0	1.17±0.42	1.88±0.71	0±0	2.09±1.02	1.23±0.67
pH end insult	7.48±0.02**	7.11±0.04	7.00±0.02	7.53±0.02^^	7.09±0.02	7.06±0.03
ABE end insult	6.00 ±0.83**	-17.24±0.76	-18.23±1.57	8.52±1.79^^	-16.31±1.05	-17.36±1.20
pCO_2 end insult	40.83±1.73	37.1±4.93	49.93±3.67	38.12±1.48	43.43±3.83	43.91±2.80

Data are mean ±SEM. ** $p<0.01$ wrt 24h HI and HI Sz groups. ^^ $p<0.01$ wrt 72h HI and HI Sz groups. LaEEG, low aEEG (<5µV).

Table 4: Spearman correlation coefficients (r_s) for the relationship between average cortical expression of p8GFAP and p13GFAP, histology and antemortem variables at 24h and 72h post-insult

Parameter examined	24h post-insult		72h post-insult	
	Correlation with p8GFAP	**Correlation with p13GFAP**	**Correlation with p8GFAP**	**Correlation with p13GFAP**
Body weight	n/s	n/s	n/s	n/s
Insult length	n/s	n/s	n/s	0.462*
Time LaEEG	n/s	n/s	n/s	0.464*
Time MABP <70% baseline	n/s	n/s	n/s	n/s
Time HR<140bpm	0.552**	n/s	n/s	n/s
pH end insult	-0.578**	n/s	n/s	-0.568**
ABE end insult	-0.426*	n/s	n/s	-0.608**
pCO_2 end insult	n/s	n/s	n/s	n/s
Neurobehaviour score 8hr	n/s	-0.414*	n/s	n/s
Neurobehaviour score 12hr	n/s	-0.421*	n/s	n/s
Neurobehaviour score 16hr	n/s	-0.417*	n/s	n/s
Neurobehaviour score 24hr	-0.467*	-0.422*	-0.506*	-0.628**
Neurobehaviour score 48hr	N/A	N/A	-0.634**	-0.681***
Neurobehaviour score 72hr	N/A	N/A	-0.432*	-0.510*
aEEG score 1hr	0.546**	0.585**	n/s	n/s
aEEG score day 1	0.626**	0.525*	0.568**	0.530**
aEEG score day 2	N/A	N/A	0.503*	0.571**
aEEG score day 3	N/A	N/A	0.584**	0.612**

N/A, data not available for this time point; n/s, not significant; * $p<0.05$; ** $p<0.01$; *** $p<0.001$.

Figure Legends

Figure 1

Western blotting using normal and pre-absorbed primary antibody solutions. A protein ~50kDa in size, representing pGFAP, was detected when the normal primary antibody solutions for p8GFAP (lane 1) and p13GFAP (lane 3) were used for immunoblotting, but the protein was not detected when pre-absorbed primary antibody solutions were used (lanes 2 and 4). Lane 5 shows representative no primary antibody control.

Figure 2

Western blotting with regular and dephosphorylated membrane shows specificity of phosphoantibody. Lane 1, untreated membrane; lane 2, dephosphorylated membrane; lane 3, no primary antibody control. pGFAP was detected on the untreated membrane (A, lane 1) but not on the dephosphorylated membrane (A, lane 2). Blots were stripped and re-exposed to film to ensure antibodies were effectively removed (B). Immunoblotting for GFAP demonstrated that regular GFAP protein was detected on the untreated membrane (C, lane 1) and the dephosphorylated membrane (C, lane 2).

Figure 3

Immunohistochemistry for GFAP and pGFAP in pig brain. A-C: Individual astrocyte from control pig brain showing immunolabelling for p13GFAP (A), GFAP (B), and merged image (C). The p13GFAP antibody immunolabelled astrocytes that co-expressed GFAP protein. D: GFAP and pGFAP were differentially expressed in the astrocyte. Arrow indicates an astrocyte process expressing only GFAP (red); double-headed arrow indicates an astrocyte process co-expressing p13GFAP and GFAP (yellow); arrowhead indicates strong expression of p13GFAP in unusual terminal dilations of the astrocyte processes. E: Immunolabelling for pGFAP (green) was observed in end-feet of astrocytes contacting blood vessels (BV). Scale bars: A-D, 10μm; E, 50μm.

Figure 4

Expression of pGFAP in control and HI pig brains. Expression of p13GFAP was observed in control brains (A) in atypical astrocytes with short processes (arrows) and in occasional astrocytes (double-headed arrow in A, and panel D) with longer processes that were atypical, that is, they had thickened, varicose processes. Expression of pGFAP in HI pig brains with mild or no damage at 72h post-insult (B) was similar to control brains – pGFAP was observed in astrocytes with short processes (arrows). pGFAP expression was upregulated in HI animals with moderate to severe brain injury at 72h post-insult (C). In these animals, expression of pGFAP was associated with astrocytes with abnormal cytoskeletal morphology (E). a, astrocyte cell body; n, neuronal cell body. Scale bars A-C, 20μm; D-E, 10μm.

Figure 5

Example western blot for quantification studies. For illustrative purposes, 5μg of total protein from piglet parietal cortex was separated by SDS-PAGE and western blotting performed using the p8GFAP antibody. Lane 1, control pig; lane 2, HI pig; lane 3, HI-seizure pig (72h post-insult). pGFAP was detected in all pig brains and appeared strongly expressed in protein sample from the HI-seizure animal.

Figure 6

Expression of p8GFAP across nine brain regions from control, HI and HI-seizure pigs at 24h and 72h post-insult. At 24h post-insult, p8GFAP expression was significantly different (Kruskal-Wallis test) between groups in the areas of frontal, parietal, temporal and occipital cortices. Post-hoc analysis (Mann-Whitney U test) determined that there were significant differences between control and HI-seizure animals (*, $p<0.05$; **, $p<0.01$) as well as significant differences between HI and HI-seizure animals (†, $p<0.05$; †† $p<0.01$). At 72h post-insult, p8GFAP expression was

significantly different between groups in the areas of frontal, parietal, temporal, occipital cortices, basal ganglia and thalamus. Post-hoc analysis determined that there were significant differences between control and HI-seizure animals (*, $p<0.05$; **, $p<0.01$) as well as significant differences between HI and HI-seizure animals (†, $p<0.05$; †† $p<0.01$).

Figure 7

Expression of p13GFAP across nine brain regions from control, HI and HI-seizure pigs at 24h and 72h post-insult. At 24h post-insult, there were no significant differences between groups in any of the brain regions analysed. At 72h post-insult, p13GFAP expression was significantly different between groups in the areas of frontal, parietal, temporal, and occipital cortices and basal ganglia. Post-hoc analysis determined that there were significant differences between control and HI-seizure animals (*, $p<0.05$; **, $p<0.01$) as well as significant differences between HI and HI-seizure animals (†, $p<0.05$; †† $p<0.01$). In basal ganglia alone, there was significantly increased expression of p13GFAP in HI animals compared with control (§ $p<0.05$).
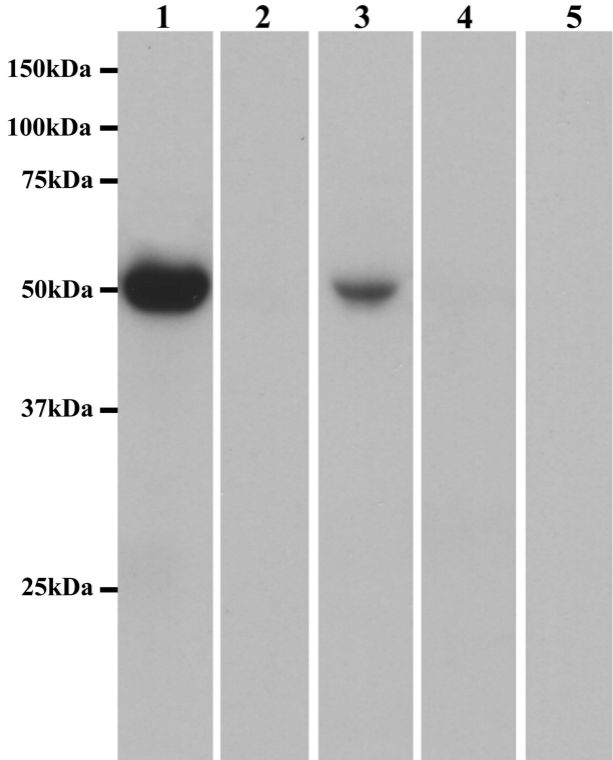
Figure 8

Relationship between increased pGFAP expression and brain injury. Increased p13GFAP expression at 72h post-insult was associated with poor aEEG score on day 1 (A), poor neurobehaviour score at 48h post-insult (B) and increased histological damage at 72hr post-insult (C). Individual data points, r_s and p-values are shown.

Figure 9

Hypoxia-ischemia and phosphorylation of GFAP. Grey boxes indicate initial events caused by HI that ultimately result in cell death. The post-HI increase in intracellular calcium and extracellular glutamate stimulate phosphorylation of GFAP, but it is unclear whether this contributes to increased cell death or is potentially part of a long-term repair/plasticity process. Phosphorylation of GFAP

causes destabilisation of the astrocyte cell process, changes in astrocyte structure and decreased regulation of the extracellular space. Phosphorylation of GFAP potentially disrupts the link between GFAP and the glutamate transporter GLAST (dotted line), which would contribute to excitotoxic cell death.

A B C D E

A Frontal Cortex

B Parietal Cortex

C Temporal Cortex

D Occipital Cortex

E Basal Ganglia

F Thalamus

G Hippocampus

H Brain Stem

I Cerebellum

Legend: Control, HI, HI Sz

y-axis (A–F): p13GFAP expression per µg protein (arbitrary units)

y-axis (G–I): p13GFAP expression per µg protein (arbitrary units)

x-axis: 24 hr, 72 hr

72hr post-insult

Legend:
- ● Control
- □ HI
- △ HI Sz

A — Average Cortical p13GFAP expression vs aEEG score on day 1
$r_s = 0.530$
$p < 0.01$
$N = 23$

B — Average Cortical p13GFAP expression vs Neurobehaviour score at 48hr
$r_s = -0.681$
$p < 0.001$
$N = 23$

C — Average Cortical p13GFAP expression vs Scaled Cortical Histology Score
$r_s = 0.681$
$p < 0.001$
$N = 23$